



## Laser surface texturing for the improvement of the press-fit joint bond strength

---

Solomon Ubani, Muhannad Ahmed Obeidi and Dermot Brabazon

EasyChair preprints are intended for rapid dissemination of research results and are integrated with the rest of EasyChair.

January 18, 2019

# Laser surface texturing for the improvement of press-fit joint bond strength

Solomon Ubani<sup>1,a</sup> Muhannad. A. Obeidi<sup>1,2,3</sup> and Dermot Brabazon<sup>1,2,3</sup>

<sup>1</sup>*School of Mechanical & Manufacturing Engineering, Dublin City University, Dublin 9, Ireland*

<sup>2</sup>*Advanced Processing Technology Research Centre APT, Dublin City University, Dublin 9, Ireland*

<sup>3</sup>*I-Form Advanced Manufacturing Research Centre, Dublin City University, Dublin 9, Ireland*

<sup>a)</sup> Corresponding author: solomon.ubani3@mail.dcu.ie

**Abstract.** The laser surface texturing has been developed for a number of applications including for enhancing the tribological properties of structural components and for improved interference fit joints. In this study, the relationship between the micro-surface textures properties and surface texture dimensions of the material such as diameter increase were determined. Optimum levels of laser power, focal position and scanning speed of the part during processing were determined. The study involved theoretical and experimental analysis of the surface response of the press-fit parts to determine optimum parameters and their corresponding changes for high joint strength and lifetime of the joint. Due to the centrifugal force, the assist gas ejection and the overlapping laser scanning tracks, the re-solidified molten surface creates a pre-defined surface texture on the material. The laser surface texturing of the interference fit pins produced an interference percentage from 4.8% to 71.4% which corresponded to insertion pin diameters from 10.2mm to 18mm. The experiments showed that the parameters had a direct correlation with joint force with values recorded between 6.84N to 184N. The analysis showed the ability to control the tensile strength of the joint structures. The experiment work performed provided a map of the relationship between the process parameters, the surface texture width and height, and the joint strengths.

**Keywords:** Tensile strength; Surface texturing; Surface modification; Fracture strength, Interference Joint.

## 1. INTRODUCTION

Laser surface texturing can be used to reduce the wear and corrosion of components used in the transport industry for piston pins, seals, bearings and cylinder liners and their use in high temperature applications [1]. In studies, it has been shown that laser surface texturing can be used for improving the distribution of surface textures to ensure the required tensile properties of the material [2]. The improvements of surfaces through laser surface texturing can result in materials with high load carrying capabilities for mechanical components [3]. This process is a low cost, high efficiency method when compared to conventional methods of fabrication of improved properties of materials. In research, there have been various studies of methods of optimizing the process of manufacture of micro-surface with high control and accuracy depending on the application.

In studies, it has been shown that surface textures with excessive height profile result in increased friction during sliding wear application when compared to polished surfaces but improvements have been observed for dimple textures with densities as low as 5% on the surface. In the manufacturing industry, the piston rings are used as a method of joining piston and cylinder liners of vehicles which have reciprocating parts and which require joining of the parts [3].



**FIGURE 1.** Piston pin used for joining the piston and cylinder liner of different inner diameters for varying joint strengths [4].

These press-fit parts are used to ensure relative motion of the parts but according to studies have caused a 40% efficiency loss in this application. These parts are used for transmitting high loads during the rotation and can cause elastic deformation to fracture the surface textures of the joint. These surface textures undergo maximum tangential forces that are larger than the shear strength of the material. The interference fit fasteners are used to reduce weight and increase the fatigue life of the parts. These interference fit joints require analysis of insertion, pullout and cyclic tensile loading and are described in the literature as a plane strain or plane stress distribution in the elastic and plastic region of steel materials.

The interference fit joints consists of shaft that is larger than a tube when inserted into the joint. The press-fit parts requires interference by the tube expansion radially and reduction of the diameter of the shaft of the joint [4]. This process is to use to ensure that stresses are uniformly distributed in the tube by the insertion of the pin into the joint. The steel materials that have brittleness due to compressive residual stresses cannot distribute the load and result in yielding and ductile properties are required for higher loads on the joint [5]. These materials with high tensile properties have a higher performance to improve the lifetime and joint strength for interference fit applications.

## 2. METHODS AND MATERIALS

### 2.1 Experimental Design

Surface texturing of the cylindrical pins was performed with a Rofin DC-015 diffusion cooled laser that has a maximum average power of 1.5kW for experiments. The laser has a focused beam with a spot size of 0.2mm and a focal length,  $f$  at 125mm in the laser system. The laser setup consisted of a translational stage moving at a speed that can be adjusted in  $x, y$  direction using the Rofin control unit and focal position,  $z_f$  that can be changed above the rotating spindle at speed on the placeholder of the laser. Therefore, the laser specification has three axes that have translational movement with an area for motion of the laser of  $1500 \times 2400$  and height of 600mm and an adjustable focal position in the range of  $\pm 150$ mm on the sample. A schematic of the laser set-up is shown in the Fig 2 below indicating the method of the process of laser surface texturing of the samples.

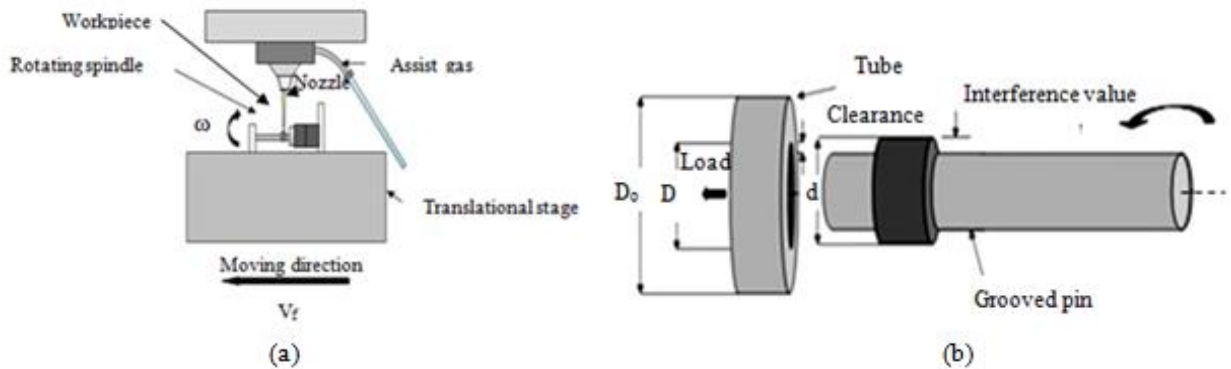


**FIGURE 2.** Schematic of (a) the laser system showing the direction used to produce laser surface texturing along the sample and the overlap of the grooves or dimples on the sample and (b) the pin and hub region of the interference fit joint.

The processing parameters and their levels for surface texturing were prepared in a Design of Experiments (DoE) format. The parameters laser power, P, focal position,  $z_f$ , and overlap ratio, OV, were chosen for the laser surface texturing and were used for a full factorial analysis of the factors and their levels for the test. The factorial experiment consisted of 3 factors and 3 levels using a Response Surface optimum design method, resulting in 27 parameter sets. The parameters and their levels were chosen to ensure melting of the material below the evaporation temperature of carbon steel of 3143°K for the experiments. The test parameters were chosen to determine the effect of this range of processing parameters for the laser surface texturing of the samples.

**TABLE 1.** The factorial design of the parameters and their levels for the laser surface texturing experiments.

Factor	Name	Units	Type	Subtype	Minimum	Maximum	Coded	Values	Mean	Std. Dev.
A	Power	W	Numeric	Continuous	300	500	-1.00 =300	1.00 =500	400	83.2
B	F.P	mm	Numeric	Continuous	-1.5	1.5	-1.00 =-1.5	1.00 =1.5	0	1.25
C	OV	%	Numeric	Continuous	-20	20	-1.00 =-20	1.00 =20	0	16.7

## 2.2 Specimen Preparation

For this study, mild steel cylindrical samples of 10 mm diameter and 60 mm length were employed during the experimental work in a 3<sup>3</sup> level full factorial DoE model. The table below shows the chemical composition of the pin and hub joint used for the laser surface texturing tests of the samples.

**TABLE 2.** Chemical composition of mild steel samples.

C	Mn	P	S	Cu	Ni	Cr	Mo	Fe
0.15-0.43	0.15-0.8	0.01-0.04	0.03-0.04	0.18-0.55	0.03-0.11	0.07-1	0.01-0.25	0.4-98.6

This mild steel material was used to fabricate the hubs using the CNC lathe machine to the dimensions of 30mm outer diameter, 10.05 inner clearance diameter and 10mm length as shown in figure 2. The hubs were chamfered at the inner diameter with a 45° taper for the insertion of the pin of the press-fit joint. The interference fit involved laser surface texturing of length of 10mm along the pin for insertion into the hub of the joint. An interference dimension was caused due to the production of the raised surface textures on the pin surface relative to the constant hub diameter [5]. The interference fit dimension percentage was calculated using the following equation:

$$\text{Interference fit size, } i = \frac{D - d}{d} \times 100\% \quad (1)$$

where D is the pin diameter and d is the diameter of the hub of the joint [5].

## 2.3 Insertion and Pull-out Test

The insertion and pull-out test were used to calculate the joint strength and were carried out using the Zwick Z-50 testing machine and using the Zwick TestXpert simulation software for determining the tensile performance of the specimens. The interference fit pin and tube were inserted into the placeholder used in measuring the tensile and compressive displacement and were controlled to 5mm/min loading rate on the samples. The interference value has an aspect ratio that affects the joint strength [5]. The surface texturing produces a groove depth to diameter ratio that is the aspect ratio for each interference value as shown below:

$$p_R = \frac{e}{w} \quad (5)$$

$$F = \frac{\pi d^2 p_R \sigma_f}{4} + \pi d l_r \tau_f \quad (6)$$

$$\text{Joint Force, } F = p_R F_a + F_n \quad (7)$$

where  $e$  is the depth of surface textures and  $w$  is the width of surface textures,  $d$  is the diameter of the pin,  $\sigma_f$  is the tensile strength of the interface,  $l$  is the length of the bonded interface of the joint and  $\tau_f$  is the shear strength of the interface. This joint force consists of the insertion and pull-out forces that are  $F_a$  the insertion force and  $F_n$  is the pullout force at the interface of the pin and tube that determines the joint strength of the material.

### 3. RESULTS

The samples were used to study the effects of the processing parameters using measurements of the diameter of the 27 samples. The pin diameters of the samples were taken using a resolution of 0.5mm of the interference value of the samples in Fig. 2 (b). The results in Fig. 4 (a) show the pin diameter with three sampling points taken on the interference length and average of each of the samples. The figure shows a clear correlation of the effects of the laser power, focal position and overlap ratio on the depth of the melt pool on the samples. It can be observed that laser power is the most significant parameter and decreases with the interference diameter of the samples and other parameters show a corresponding increase with the pin diameter of the specimens.

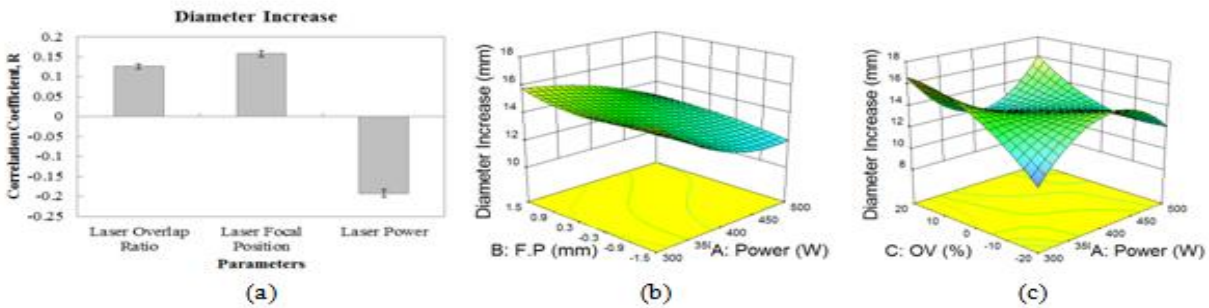


**FIGURE 3.** Graph of the (a) correlation coefficient of diameter due to the effects of parameters on the sample (b) surface plot of interaction of laser power and focal position and (c) surface plot of interaction of overlap ratio and laser power on the sample.

The processed samples from the factorial experiments of the different laser treatments on the response were carried out to obtain a relationship of the parameters on the diameter increase due to the height of the interference and the surface roughness effect on the contact area between the interference fit parts.

The table 3 below shows the effects of the changes of laser power on the increase of the pin diameter,  $i$  and their corresponding residence time and laser irradiation absorbed on the surface of the sample. The results indicate a relation of laser power on the measured depth of interference, at a constant scanning speed, spot size on the sample.

The table 4 below shows the effects of the changes of focal position on the width of the surface textures and residence time and laser irradiation of the sample. The table indicates that the size of the melt pool width,  $w$ , increased as the focal position was increased. In this table, the angle of the texture,  $\alpha$ , with respect to the pin longitudinal axis is also represented.

**TABLE 3.** Effect of the laser power on surface morphology, residence time and laser irradiance of the sample.

P (W)	$V_s$ (mm/min)	$d$ (mm)	$i$ (mm)	$t$ (ms)	$I_o$ (kW/mm <sup>2</sup> )
300	1200	0.2	4.47	1571	11.3
400	1200	0.2	3.27	1571	12.6
500	1200	0.2	8	1571	9.34

**TABLE 4.** Effects of the focal position and processing parameter on the topography of the surface textures, processing time and laser absorbed irradiance on the sample.

$z_f$ (mm)	PRF (Hz)	Duty Cycle(%)	P (W)	$w$ (mm)	$\alpha$ (°)	$t$ (sec)	$I_o$ (kW/mm <sup>2</sup> )
-1.5	100	80	400	0.428	2.02	1571	12.62
0	100	80	400	0.476	1.75	1571	12.58
1.5	100	80	400	0.524	1.35	1571	9.34

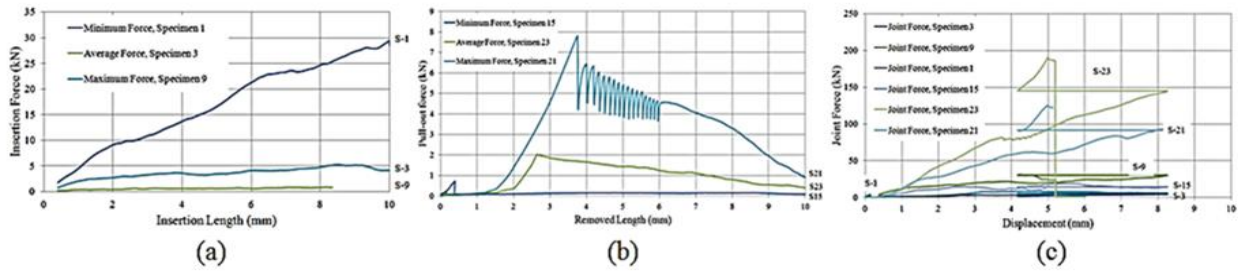


**FIGURE 4.** Graph of the (a) insertion force for Samples 1, 3, 9, (b) pull-out force for Samples 15, 21, 23 (c) joint force for the Samples, 1, 3, 9, 15, 21, 23 showing the range of values of the experiments.

Fig. 4 (a) below shows the samples chosen with different interference values of 41.6%, 14.3%, and 22.3% that had maximum, average and minimum insertion forces during constant loading on the tensile testing machine of the samples. The graph was observed to have a range of insertion force obtained from the laser surface texturing tests of  $7.93 \pm 19.27$  kN showing significant variability of the processing parameters during insertion of the cylinder from the average of the results. The results of the ANOVA show a 95% confidence interval of the parameters on the response and shows fit of the model and results of the samples.

The results shown in Fig. 4 (b) are the pull-out forces during the disassembly of the fastener pin from the hub and the range of the values of the specimens that had minimum, average and maximum forces involved on the samples. The graph indicates a lower variation across each of the samples with a range of pull-out force obtained of  $2.25 \pm 0.81$  kN and it can be observed a high amount of control of parameters on the response of the samples. The samples had a range of interference sizes of 30.2%, 34.8%, 29.6% and show the steel material had adequate interference for a high pull-out force of the pin on the hub assembly of the joint. The samples with the lowest interference value results in lack of pull-out force due to the removal of the pin from the hub joint.

Fig. 4 (c) shows the calculated response of the joint force due to insertion and removal of the pin from the joint. The results were used to determine a range of joint strength from 6.84kN to 184kN of the samples. The results were studied in ANOVA and showed that factor A, B and their interactions AB, AC are significant on the surface response. The response can be observed to have a decrease with the overlap ratio and shows that this parameter is significant in the strength of the joint holding the pin in the hub assembly of the joint. The processing parameters such as the laser power and focal position were observed to produce the peak in the joint strength at laser powers of 400W and focal position on the surface of the sample.

## 4. DISCUSSION

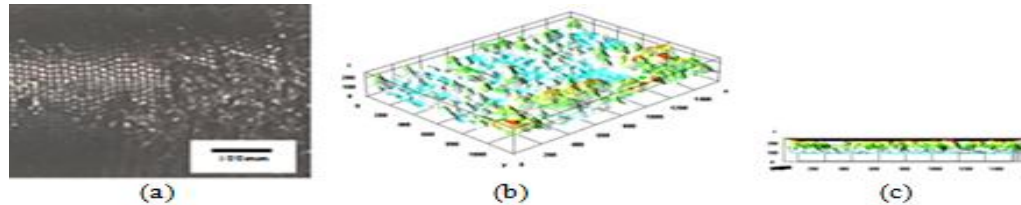
### 4.1 Effects of Laser Processing on Insertion and Pull-out of the Joint

Fig. 4 (a) shows that sample 1 was obtained for laser power of 500W, overlap ratio of -20% and focal position of -1.5% below the surface of the material. The parameters significant in this result were the laser power and focal position that affect this heat input and resulted in this increase of the pin diameter of the samples. Sample 9 had the lowest insertion force of assembly with fracture of surface textures and loss of load at 8.33mm along the insertion length due to a high interference size but low surface roughness for gripping and assembly of the pin in the hub of the joint. This sample had a grooved pin produced with constant focal position as Sample 1 but with an overlap ratio of 0% and laser power of 400W that results in an adequate diameter increase but due to lack of overlap of grooves over each other results in low gripping performance of the samples. This results indicates the surface roughness is an important property in the gripping and assembly of the samples in interference fit applications.

Fig. 4 (b) shows the sample 21 had the highest pull-out force but from the graph it can be observed variability due to the contact that occurs at 3.74mm and ends at 6.05mm that indicates some friction due to the steel contact between the surface after it reaches its peak value of the pull-out force of 7.81kN at the centre of the removal length of the samples. In the literature it was said that the maximum hoop stress due to the joining of parts occurs at the centre due to the elastic and plastic deformation of expansion of the pin in the hub cavity of the joint. This result was obtained for processing parameters at the levels of laser power of 300W, overlap ratio of 20% and focal position on the surface of the sample. This sample indicates that laser power and focal position were significant in producing

adequate diameter increase of pull-out force of the samples and the overlap ratio of the surface textures over each other on the sample. This processing parameter resulted in a grooved pin with high surface roughness and a corresponding high pull-out force of removal of the pin from the hub of the joint.

The joint strength in Fig 4 (c) of the fastener pin and the hub shows for aspect ratios such as specimen 9 did not have a uniform stress distribution and had interference size of 28.7% and aspect ratio of 5.73 of the grooves of the pin on the inner diameter of the tube of joint. The surface textures produced at this interference value causes loss of joint strength and separation of assembly of joint. The specimen 23 has aspect ratio that is larger of 8.53 corresponds to an interference size of 53.3% that produced high stresses of the pin in the hub and reduction of joint strength.



**FIGURE 5.** Sample 23 which had the highest joint strength showing (a) low magnification image (100mm) (b) high magnification image (100 $\mu$ ) using microscope at a resolution of 0.1 $\mu$ m of material.

Fig. 5 (a) shows a high reflective surface for Sample 23 that had a uniform distribution of surface textures and had crack formation and the highest joint strength of the samples. The samples not within these ranges had an increase in joint strength but samples change from positive to negative strength that separates the assembly of the joint. Therefore steel materials between these limits do not reduce joint strength. The interference fit joints showed a high joint quality that undergoes deformations to increase the contact pressure of the parts. The results show that the joint strength and fatigue properties produced an improvement on the strength of the joint.

## 5. CONCLUSION

Laser surface texturing for applications in press-fit of piston and cylinder liners in the transport industry were studied using tensile tests of the samples. The laser parameters used in this study were the laser power, overlap ratio and focal position that obtained a high joint strength by increasing the interference value on the specimens. The interference size was obtained between negative interference of 3.18% and positive interference of 71.4% on the pin when inserted into the tube of the joint.

These experiments were used to improve the joint strength and fatigue properties for maximum bond strength of the joint. The interference fit joint obtained a high joint strength and was a combination of the high insertion and pull-out force of the specimens. The joint strength was optimized to determine improvements on the press-fit joint.

The laser surface texturing tests show a significant improvement of the performance of vehicles for high loading capacity and service time of the parts of the joints. This process can be used to obtain specific required properties of the joint for high joint strength interference fit applications.

## 6. ACKNOWLEDGEMENTS

The author gratefully acknowledges Dublin City University for use of the research facilities for this project.

## 7. REFERENCES

1. [K. Jones, S. Schmid, Experimental Investigation of Laser Texturing and Its Effect on Friction and Lubrication, Procedia Manufacturing Volume 5, Pages 568–577 \(2016\).](#)
2. [M. Obeidi, E. McCarthy, D. Brabazon, Methodology of laser processing for precise control of surface micro-topology, Surface & Coatings Technology 307, 702–712 \(2016\).](#)
3. [D. Li, X. Chen, C. Guo, J. Tao, C. Tian, Y. Deng, W. Zhang, Micro surface texturing of alumina ceramic with nanosecond laser, Procedia Engineering 174, 370 – 376 \(2017\).](#)
4. [L. Ba, Z. He, Y. Liu, G. Zhang, Analysis of piston-pin lubrication considering the effects of structure deformation and cavitation, Journal of Univ-Sci A \(Appl Phys & Eng\), 16\(6\):443-463\(2015\).](#)
5. [Y. Bi, J. Jiang, Y. Ke, Effect of interference fit size on local stress in single lap bolted joints, Advances in Mechanical Engineering, Vol. 7\(6\) 1–12 \(2015\).](#)
6. [N. Tada, T. Tanaka, T. Uemori, T. Nakata, "Evaluation of Thin Copper Wire and Lead-Free Solder Joint Strength by Pullout Tests and Wire Surface Observation.," Crystals, 7, 255 \(2017\)](#)
7. [W. Steen, "Laser material processing" 2nd ed, Springer \(1998\).](#)